Highlights

The impact of steric repulsion on the total free energy of electric double layer capacitors

Dagmawi B. Tadesse, Drew F. Parsons

- We derived a steric chemical potential for a composite diffuse layer (CDL) model from net forces on an ion in equilibrium.
- We derived an analytical expression for the total free energies of the system in terms of the physical parameters of the electrode, electrolyte ions and the solvent.
- The analytical expression of total free energy matches the Bikerman steric model well.
- The steric contribution introduces an ion-size specific effect to the totoal free energy of a supercapacitor.
- We studied the steric energy is comparable to the electrostatic energy, indicating that $1/2CV^2$ does not correctly represent the energy of a supercapacitor.

The impact of steric repulsion on the total free energy of electric double layer capacitors

Dagmawi B. Tadesse[a], Drew F. Parsons[b,a]

[a]Discipline of Physics, Chemistry and Mathematics, C'SHEE, Murdoch University, 90 South St, Murdoch, 6150, WA, Australia
[b]Department of Chemical and Geological Sciences, University of Cagliari, Cittadella Universitaria, Monserrato, 09042, Cagliari, Italy

ARTICLE INFO

Keywords:
Supercapacitor
Electric Double Layer Capacitor
Modified Poisson-Boltzmann
Steric Interaction
Steric Layer
Composite Diffuse Layer
Total Free Energy

ABSTRACT

We present an analysis of the total free energy of a supercapacitor modelled with a composite diffuse layer (CDL) formed by a steric repulsive potential. The steric potential is modelled with a simple approximation to the Bikerman steric potential, enabling derivation of an analytical expression for the total free energy of the supercapacitor in terms of the size and valency of the electrolyte counterions and electrode potentials. The analytical expression for the total free energy of the supercapacitor matches the exact numerical Bikerman calculation at high potential with relative error close to 1%. This provides an upper bound over the more accurate Carnahan-Starling model. A maximum upper bound for the energy is also provided in the limit where bulk concentrations approach the ion concentration cap. We also analyze the relative contribution of the steric interaction to the total free energy. At large voltages, the steric free energy is comparable in magnitude to that of the electrostatic free energy, and introduces ion-size effects in the energy of the supercapacitor. Consequently at high potentials the total free energy exceeds (doubles) the classical energy $\frac{1}{2}CV^2$, indicating that this formula does not correctly describe the available stored energy from the experimentally measured capacitance.

1. Introduction

Due to their superior power density over the likes of Li-ion batteries, electric double layer capacitors (EDLCs), a class of supercapacitor also known as ultracapacitors, are becoming widely used in many energy storage applications. In contrast to batteries where there is a chemical reaction taking place between the electrode and the electrolyte solution, the EDLCs store energy using an electric double layer formed by physically adsorbing ions to the surface of an electrode, hence the name electric double layer capacitors.

The performance, mainly capacitance and energy, of these energy storage depend on the structure of the EDLs at the surface of the electrodes. At thermal equilibrium, the EDL structure in EDLC can be described using Poisson-Boltzmann (PB) theory. This theory is a mean field theory which neglects the steric effect, treats ions in solution as point-like particles and considers the solvent as a structureless continuous medium represented by a macroscopic dielectric constant. Although conventional PB theory is successful in lower electrostatic potential regimes, this model is known to grossly over-predict the concentration of counterions near highly charged surfaces when steric effects are neglected, electrolyte ion size and shape unaccounted for [1, 2] and explicit solvent structure overlooked. As a result PB theory predicts an unbounded capacitance and unphysically high total free energy of the EDLC at typical electrode potentials of 1V.

Stern was the first to recognize the limitation of point-like ions in 1924 [3]. Since then there have been numerous efforts made to account for the effect of finite ion sizes on the structure [4, 5, 6, 7, 8, 9, 10, 11] and the total free energy of EDL [12, 13, 14, 15]. There were also efforts to modify PB going beyond accounting for finite ion sizes to address effects of shape and hydration layers of the electrolyte ion [16, 17, 18], structure and physical properties of the solvent [19, 20, 21, 22, 23] on the structure and energy of EDL. A concise review on the effects ion and solvent on the structure and total free energy of EDL is given in [24]. More recently, Fileti [25] calculated the energy of EDLCs using approaches he referred as thermodynamic and conventional electrostatic approaches. His thermodynamic approach used the total free energy of the EDL whereas for the conventional electrostatic approach, he computed the differential capacitance from the electrostatic potential and used the conventional $\frac{1}{2}CV^2$ to calculate the stored energy. There are

*drew.parsons@unica.it
ORCID(s):

also number of experimental works that uses the conventional electrostatic approach where they calculate the stored energy of an EDLC from experimentally measured capacitance [26, 27].

In this study, our main result is the derivation of an analytic expression for total free energy of a supercapacitor, comprised of the electrostatic, configuration entropy and steric energy of ions. We present an approximate model of the steric potential that treats ions as point particles at low potentials and finite-sized hard-spheres for potentials larger than a threshold, providing an approximation to the Bikerman steric potential [4]. We then compute the total free energy of a supercapacitor and compare our findings with the electrostatic approach of $\frac{1}{2}CV^2$. Importantly, we studied the impact of the steric interactions on the total free energy of an EDLC. More complex but accurate models such as the Carnahan-Starling (CS) steric potential [6, 28, 29, 30] require solving a highly nonlinear modified PB equation, or oscillatory ion-ion correlations requiring the solution of integral equations [31, 32]. An analytical expression for the total free energy, while likely to overestimate the total free energy, immensely simplifies the analysis by avoiding the nonlinearity inherent to the Carnahan-Starling model or the integral equation methods, and the introduction of ion size effects provides a framework to start understanding Hofmeister (specific ion) effects in electrochemical systems [33, 34].

2. Steric Interaction and EDL

Consider a flat-surfaced electrode with potential $\Phi_{s\alpha}$ immersed in electrolyte solution. The chemical potential, μ_i, of the i^{th} ion at any position in the solution is given by

$$\mu_i(x) = \mu_i^{\text{en}}(x) + \mu_i^{\text{ex}}(x) \tag{1}$$

where $\mu_i^{\text{en}} = k_{\text{B}}T\ln(\chi_i)$ is the entropic chemical potential, k_{B} is Boltzmann constant, T is temperature and χ_i is mole fraction. $\mu_i^{\text{ex}} = \mu_i^{\text{el}} + \mu_i^{\text{st}}$ is the excess chemical potential, in which we include the electrostatic component μ_i^{el} and, importantly, a steric interaction μ_i^{st}. $\mu_i^{\text{el}} = z_i e\Phi$, where z_i is the valence number of the i^{th} ion, e is the elementary charge, Φ is the electrostatic potential.

Through an excluded volume approach Bikerman proposed the effect of steric interactions of finite sized ions [4]. The generalized non-ion size specific steric interaction, related to solvent entropy [9], is given by

$$\mu^{\text{st,bik}} = -k_{\text{B}}T\ln(1-\varphi) \tag{2}$$

where $\varphi = \sum_i c_i v_i$ is the volume fraction of the ions, c_i and v_i are the concentration and volumes of the i^{th} ion. A more sophisticated and accurate steric interaction was given by non-ion size specific Carnahan-Starling (CS) model [6] as

$$\mu^{\text{st,cs}} = k_{\text{B}}T\frac{\varphi(8-9\varphi+3\varphi^2)}{(1-\varphi)^3} \tag{3}$$

The CS model is extended to account for mixtures of unequal ion sizes in Boublik-Mansoori-Carnahan-Starling-Leland (BMCSL) model [29]. In spite of the accuracy of these models, their nonlinearity in the dependence on ion concentrations makes these advanced models challenging to solve.

We consider an approximate steric expression derived from a steric force, $f_i^{\text{st}} = -\nabla\mu_i^{\text{st}}$, which represents a short range interaction that prevents ion overlap. In thermal equilibrium, the resultant force due to the sum of the electrostatic force, $f_i^{\text{el}} = -\nabla\mu_i^{\text{el}}$, the entropic force, $f_i^{\text{en}} = -\nabla\mu_i^{\text{en}}$, and the short range steric force on an ion must equal zero, i.e. $0 = f_i^{\text{el}} + f_i^{\text{en}} + f_i^{\text{st}} = -\nabla\left(\mu_i^{\text{el}} + \mu_i^{\text{en}} + \mu_i^{\text{st}}\right)$. This is equivalent to taking the total chemical potential to be constant with respect to position under the condition of thermal equilibrium. By setting the chemical potential at any position equal to that in bulk where the ion concentration is $c_{i\infty}$, we thereby obtain an the expression for the steric chemical potential as $\mu_i^{\text{st}} = -k_{\text{B}}T\ln\left(c_i/c_{i\infty}\right) - \mu_i^{\text{el}}$, where c_i is the ion concentration. Since the steric force is a short range interaction, it is activated when the concentration surpasses a threshold, c_i^{cap}. In this paper, we used ion volumes V_i determined by quantum chemical calculations [35] to estimate the concentration cap as $c_i^{\text{cap}} \sim 1/V_i$. Thus the steric term is turned on when the threshold, μ_i^{cap}, controlled by ion size, is exceeded. That is, we define the steric potential as [36, 37]

$$\mu_i^{\text{st}} = \begin{cases} \mu_i^{\text{cap}} - \mu_i^{\text{el}}, & \text{if } \mu_i^{\text{el}} < \mu_i^{\text{cap}} \\ 0, & \text{otherwise} \end{cases} \tag{4}$$

where $\mu_i^{\text{cap}} = -k_{\text{B}}T \ln(c_i^{\text{cap}}/c_{i\infty})$. In contrast to the Bikerman Eq.(2), Eq.(4), is only active when a threshold is passed and therefore can be taken as an approximation at high potential regime. The advantage of this model is its simplicity and accuracy at high potential. In thermal equilibrium, for a chemical potential given by Eq.(1), the Poisson-Boltzmann equation will have the form

$$-\nabla^2\Phi(x) = \sum_i^N \frac{ez_i c_{i\infty}}{\varepsilon_0\varepsilon_s} \exp\left(-\frac{\Delta\mu_i^{\text{ex}}}{k_{\text{B}}T}\right) \tag{5}$$

where ε_0 is vacuum permittivity, ε_s is the dielectric function of the solvent medium, k_{B} is Boltzmann constant, $\Delta\mu_i^{\text{ex}}$ is the change in the excess chemical potential of the ion from the reference bulk.

The differential capacitance for this model is given by Ref[10]

$$C = \begin{cases} \dfrac{\varepsilon}{\lambda_D}\cosh\left(\dfrac{ze\Phi_s}{2k_{\text{B}}T}\right), & \text{if } \Phi_s < \Phi_c \\ \dfrac{\frac{1}{\sqrt{2\nu}}\frac{\varepsilon}{\lambda_D}}{\sqrt{\left(1-\frac{\nu}{2}\right)^2 + \frac{ze|\Phi_s|}{k_{\text{B}}T} - \ln\left(\frac{2}{\nu}\right)}}, & \text{otherwise} \end{cases} \tag{6}$$

where $\nu = 2c_\infty/c^{\text{cap}}$ and $\lambda_D = (\varepsilon_0\varepsilon_s k_{\text{B}}T/\sum_i z_i^2 e^2 c_{i\infty})^{1/2}$ is the Debye-length. For low electrode potential regime, $\Phi_s < \Phi_c$, where $\Phi_c = \mu^{\text{cap}}/ze$ it the threshold potential where the steric effect comes into play, the model treats the ions as point particles and the capacitance reduce to the Gouy-Chapman capacitance. At high potential regime, the

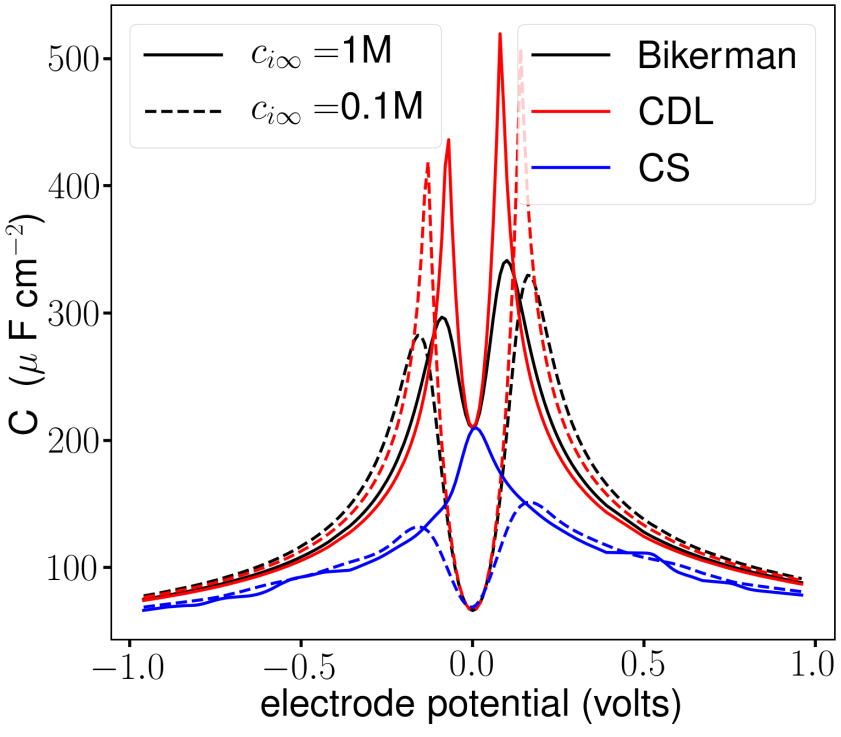

Figure 1: Comparison of single-electrode differential capacitance of Li^+ and PF_6^- ions in propylene carbonate for CDL, Bikerman and CS models.

capacitance is ion-size specific and it converge to that of the Bikerman capacitance, while the CS capacitance remain

significantly lower as shown in Fig.1. For further details on the differential capacitance of the CDL, Bikerman and CS models refer to Ref[10, 24, 28, 29]. Here we are mainly interested on the steric effect on the energy of EDLCs.

3. Total Free Energy

The total free energy F is composed of entropic, electrostatic, and steric contributions [12, 38, 39],

$$F = F_{\text{en}} + F_{\text{el}} + F_{\text{st}} \tag{7}$$

where F_{en} is the ionic entropic contribution (configuration entropy),

$$F_{\text{en}} = k_{\text{B}}T \sum_i \int dx \left[c_i(x) \ln \frac{c_i(x)}{c_{i\infty}} \right] \tag{8}$$

F_{el} is the electrostatic contribution given by

$$F_{\text{el}} = \frac{\varepsilon_0 \varepsilon_s}{2} \int dx \, |\nabla \Phi(x)|^2 \tag{9}$$

and the steric contribution, F_{st}, given by

$$F_{\text{st}} = \sum_i \int dx \, \Delta\mu_i^{\text{st}}(x) c_i(x) \tag{10}$$

where $\Delta\mu_i^{\text{st}}$ is the change in the steric chemical potential of the ion from the reference bulk.

For electrode potential, $\Phi_{s\alpha} > \Phi_{c\alpha}$, Eq.(5) describes a composite diffuse layer (CDL), with steric layer thickness, H_α and electrode charge density σ_α, where α marks the electrode and corresponding counterion with respect to the charge of that electrode. For z:z symmetric electrolytes, they are respectively given by Eq.(21) and Eq.(22) of Ref[10] as

$$\begin{aligned} H_\alpha &= \lambda_D \sqrt{2\nu_\alpha} \left[-1 + \frac{\nu_\alpha}{2} + \sqrt{\left(1 - \frac{\nu_\alpha}{2}\right)^2 - \frac{z_\alpha e \Phi_{s\alpha}}{k_{\text{B}}T} - \ln \frac{2}{\nu_\alpha}} \right] \\ \sigma_\alpha &= -2\rho_\alpha^{\text{bulk}} \lambda_D \sqrt{\frac{2}{\nu_\alpha} \left[\left(1 - \frac{\nu_\alpha}{2}\right)^2 - \frac{z_\alpha e \Phi_{s\alpha}}{k_{\text{B}}T} - \ln \frac{2}{\nu_\alpha} \right]} \end{aligned} \tag{11}$$

where z_α is the valence of the counterion, $\rho_\alpha^{\text{bulk}} = z_\alpha e c_\infty$ is volume charge density at bulk. From Eq.(11), for increasing surface potential, $\Phi_{s\alpha}$, the steric layer H_α also increases. And at the limit of high potential, the steric layer, H_α becomes very thick relative to the tail of the Debye length. Thus the EDL can be approximated as a step function near the electrode, with counterion concentration given by

$$c_\alpha(x) = \begin{cases} c_\alpha^{\text{cap}}, & \text{if } x \le H_\alpha \\ c_{\alpha\infty}, & \text{otherwise} \end{cases} \tag{12}$$

The electric field in this steric layer is

$$E_\alpha(x) = \frac{\sigma_\alpha}{\varepsilon_0 \varepsilon_s} + \frac{\rho_\alpha^{\text{cap}}}{\varepsilon_0 \varepsilon_s} x \tag{13}$$

where $\rho_\alpha^{\text{cap}} = z_\alpha e c_\alpha^{\text{cap}}$ is the capped volume charge density of the counterion. z_α is the valence number of the counterion. The potential in the steric layer can be calculated from the electric field and is given by

$$\Phi_\alpha(x) = \Phi_{s\alpha} - \frac{\rho_\alpha^{\text{cap}}}{2\varepsilon_0 \varepsilon_s} x^2 - \frac{\sigma_\alpha}{\varepsilon_0 \varepsilon_s} x \tag{14}$$

Outside the steric layer, both the electric field and the potential are relatively small and can be taken zero as in the bulk. Using these assumptions, Eq.(12) and Eqs. (8) to (10), the corresponding free energy components for this high potential limiting case can be approximated for a two electrode system as

$$F_{\text{en}} = k_{\text{B}}T \sum_{\alpha} \left[c_{\alpha}^{\text{cap}} \ln \frac{c_{\alpha}^{\text{cap}}}{c_{\alpha\infty}} \right] H_{\alpha} \tag{15}$$

for the entropic contribution, with the sum over α indicating that all electrodes are counted in the total. The electrostatic contribution is approximated by

$$F_{\text{el}} = \frac{1}{2\varepsilon_0\varepsilon_s} \sum_{\alpha} \left[\frac{(\rho_{\alpha}^{\text{cap}})^2}{3} H_{\alpha}^3 + \sigma_{\alpha}\rho_{\alpha}^{\text{cap}} H_{\alpha}^2 + \sigma_{\alpha}^2 H_{\alpha} \right] \tag{16}$$

Accordingly, the steric free energy is given by

$$F_{\text{st}} = \sum_{\alpha} \left[\mu_{\alpha}^{\text{cap}} c_{\alpha}^{\text{cap}} - \rho_{\alpha}^{\text{cap}} \left(\Phi_{s\alpha} - \frac{\sigma_{\alpha} H_{\alpha}}{2\varepsilon_0\varepsilon_s} - \frac{\rho_{\alpha}^{\text{cap}} H_{\alpha}^2}{6\varepsilon_0\varepsilon_s} \right) \right] H_{\alpha} \tag{17}$$

For a two electrode system with a potential difference V, one consequence of the ion size difference between anion and cation is that the electrode does not split the voltage equally ($\Phi_{s\alpha} \neq V/2$) [40]. In order to calculate the electrode potentials from the potential difference, charge conservation across the electrodes must apply, with the total sum of the charge densities over all electrodes being zero, i.e $\sigma_+ = -\sigma_-$. From this condition the electrode potential follows as

$$\begin{aligned} \Phi_{s1} = \frac{k_{\text{B}}T}{e(z_2\nu_1 - z_1\nu_2)} \Bigg[& \frac{z_2\nu_1 e}{k_{\text{B}}T} V + \nu_1 \left(1 - \frac{\nu_2}{2}\right)^2 \\ & - \nu_2 \left(1 - \frac{\nu_1}{2}\right)^2 + \nu_2 \ln \frac{2}{\nu_1} - \nu_1 \ln \frac{2}{\nu_2} \Bigg] \end{aligned} \tag{18}$$

and the counter electrode potential will be $\Phi_{s2} = \Phi_{s1} - V$. For a single electrode, only the counterion contributes to the free energy and the summations over the ions are dropped.

Eqs. (15) to (17) are analytical approximations of Eqs. (8) to (10), respectively valid for potentials beyond the steric limit. They can be used to estimate the total free energy of an EDL system only from the physical parameters used such as bulk concentration of the solution, the dielectric constant of the solvent, the ion sizes and electrode potential without the need to solve PB.

4. Results & Discussion

In the discussion below, we investigate how the Bikerman and CDL model compare against each other and explored the potential regime where the components of the free energy dominates. We also calculated the corresponding free energy approximation given by Eqs. (15) to (17) and show how well it agrees with the two models. Although it is well established that the energy of an electric-double layer capacitor/supercapacitor is not linear with its capacitance, $E = \frac{1}{2}CV^2$ is conventionally being used to calculate the energy of such systems from experimentally measured capacitance. We also investigated how well this expression matches that of the the total free energy.

We used $LiPF_6$ salt which is commonly used in energy storage application. We used hydrated-lithium ion radius of 2.82Å and 2.54Å for PF_6^- ion. The solvent is chosen to be propylene carbonate and bulk ion concentrations taken as $c_\infty = 1$M. We note that the dielectric constant of the solvent is non-uniform over the solution and the effective value is less than the static dielectric constant [41]. However for this work we restrict ourselves to a uniform dielectric constant value of $\varepsilon_s = 66.14$. Eq.(5) is solved numerically by Finite Element methods using FEniCS [42] apply the Bikerman (Eq.(2)) and approximate (Eq.(4)) steric potentials, for different electrode potentials. The free energies are computed by integrating the electrostatic potentials and ions concentration obtained numerically, using Eqs. (8) to (10) for Bikerman and CDL models. For comparison, we also evaluate the Carnahan-Starling (CS) model (Eq.(3)), which is known to generally provide good agreement with Monte Carlo simulations of the electric double layer structure [30, 43]. We resolve the nonlinear relationship between electrostatic potential and total solute volume fraction applying an algorithm suggested by Chen, Dou and Zhou to (adapting Eq.3.8 in Ref.[44]).

Table 1
Ion properties: hard-sphere radius R_i, concentration cap c_i^{cap} and steric threshold potential $\Phi_{c\alpha}$ at 298K. X^- is an idealized anion with size chosen such that its concentration cap equals bulk concentration 1M.

Ions	R_i(Å)[a]	c_i^{cap} (M)	$\Phi_{c\alpha}$ (mV)
Li^+	2.82	18	-74
Cl^-	2.05	46	98
BF_4^-	2.30	33	90
PF_6^-	2.54	24	82
ClO_4^-	2.39	29	87

[a] Hard-sphere radii evaluated using radii of Gaussian spatial distributions of ions [35, 45].

We find that the total free energy and its components from CDL are in good agreement with that of the Bikerman model for potential above the steric potential threshold while the free energy from CS remains lower as shown in Fig.2. For small volume fractions, $0 < \varphi \ll 1$, the CS steric potential is roughly 8 times that of the Bikerman steric potential ($\mu^{\text{st,cs}} \approx 8\mu^{\text{st,bik}}$). For larger volume fractions, $0 \ll \varphi < 1$ then $\mu^{\text{st,cs}} \gg \mu^{\text{st,bik}}$. Owing to the stronger CS steric potential, the build up of counter-ions near the electrode is suppressed in the CS model relative to that of the Bikerman model, resulting in a relatively lower capacitance and total free energy.

For potentials below the steric threshold, the relative error between CDL and Bikerman increased up until the threshold. That is due to the increase in the steric effect in the Bikerman model which is not accounted for in the CDL model for low potential regime. The free energy of the CDL converges to that of the Bikerman model after the steric potential threshold, with relative error well below 1% for an electrode potential of 1V. Suppression of ion concentrations under the CS model results in a total free energy that reaches a magnitude around two thirds of that from the CDL model.

Table 2
Relative error of the analytical free energy approximation at the given concentration

Model	$c_{i\infty} = 0.01$M	$c_{i\infty} = 0.1$M	$c_{i\infty} = 1$M
Bikerman	4.5	2.4	1
CDL	5.9	3.1	1.1

The analytical approximations Eqs. (15) to (17) of the free energy also match those two models for potentials above the steric threshold as shown Fig.3(a) with relative error of 5% at 0.5V for Bikerman model and 0.4V for CDL. At 1V we have relative error of 1% to Bikerman and 1.1% to CDL. This approximation further matches those models for higher potential and bulk concentration as shown in Table 2 and Fig.3(b). This makes the analytical approximations very important for estimating the energy of EDLCs where the working potential and concentration is very high.

When it comes to the components of the free energy, for potentials lower than the steric threshold potential $\Phi_{c\alpha} = \mu_\alpha^{\text{cap}}/z_\alpha e$ (typically 50–200 mV, see Table 1), only the entropic and electrostatic components contribute to the total free energy. As shown in Fig.5, in this low potential regime, irrespective of the bulk concentration, the total free energy is approximately equal to $\frac{1}{2}CV^2$, where C is the total capacitance of the two electrodes system and V is the potential difference between the two electrodes. It is important to note, however that the $\frac{1}{2}CV^2$ here is not purely electrostatic, with the entropic contribution contributing equally to the total free energy. For potentials beyond the steric threshold ($\Phi_{s\alpha} > \Phi_{c\alpha}$), the total free energy exceeds $\frac{1}{2}CV^2$ due to the added contribution of the steric component. At the same time, when $\Phi_{s\alpha} \gg \Phi_{c\alpha}$, the electrostatic component F_{el} and the steric component F_{st} are both in the order of $\frac{1}{2}CV^2$ while the entropic contribution F_{en} is becomes relatively less significant. In this regime, it is fair to say that only the electrostatic component is almost equal to $\frac{1}{2}CV^2$ as shown in Fig.5 (Bottom Right). As a result if $E = \frac{1}{2}CV^2$ is used to calculate energy, a significant component F_{st} of the total energy is unaccounted for, with the expression only being valid in the low potential regime.

The steric free energy is active above the steric threshold, with both the steric and electrostatic free energies increasing as the potential difference increases. By contrast, up until the steric threshold, the entropic contribution

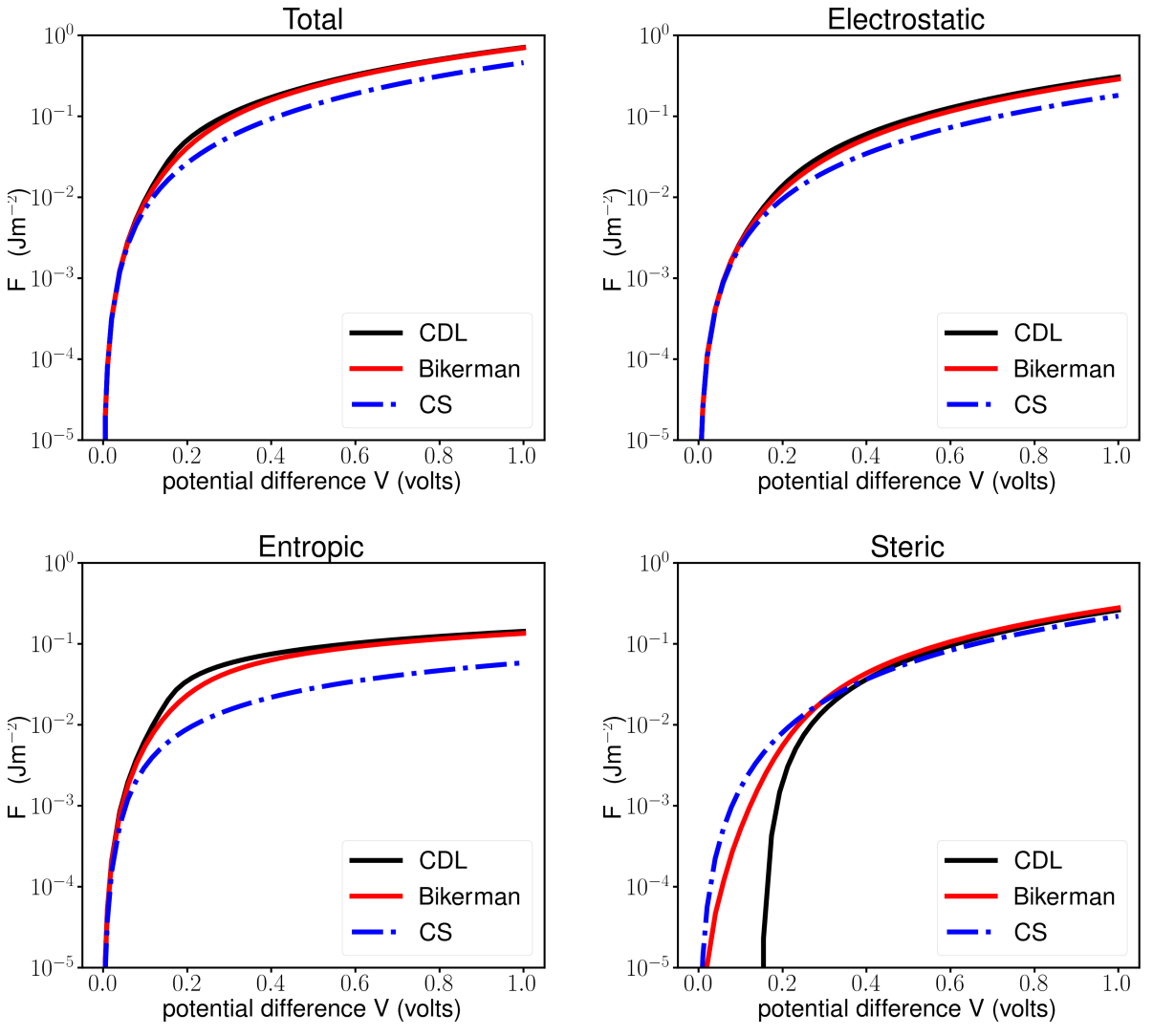

Figure 2: Comparison of the total free energy and the respective components of the CDL, Bikerman and CS models. 1M $LiPF_6$ used.

increases with increasing potential difference, owing to the increasing concentration in the adsorption layer. Beyond the steric threshold, ion concentration caps lock the entropic contribution as shown in Fig.4(a), and its relative contribution to the total free energy declines as shown in Fig.4(b). All the components of the free energy increase with increasing potential, as shown in Fig.4(a).

From log-log plots on Fig.5, the slope of the graphs indicates the power relationship between the free energies and potential. As it can be seen, the free energies have distinct slopes before and after the steric threshold with the exception of the electrostatic component. The electrostatic free energy has a slope of ~ 2 throughout the potential, which indicates $F_{\text{el}} \propto V^2$. For the total free energy, the relationship is approximately $F \propto V^2$ for potentials below the threshold. However for potentials above the threshold the relationship becomes roughly $F \propto V^{3/2}$.

In the limit of high bulk concentration where the bulk concentration approaches the concentration cap of the counterion, $c_\infty = c^{\text{cap}}$, the analytical equations derived above will reduce to simplified forms. The limit is not entirely consistent since cations and anions will generally have different concentration caps (different sizes), and in any case the concentration caps are likely to exceed solubility limits. Nevertheless the limiting expressions are useful for establishing an upper bound for the total free energy. For a single electrode system, the steric potential becomes identical to

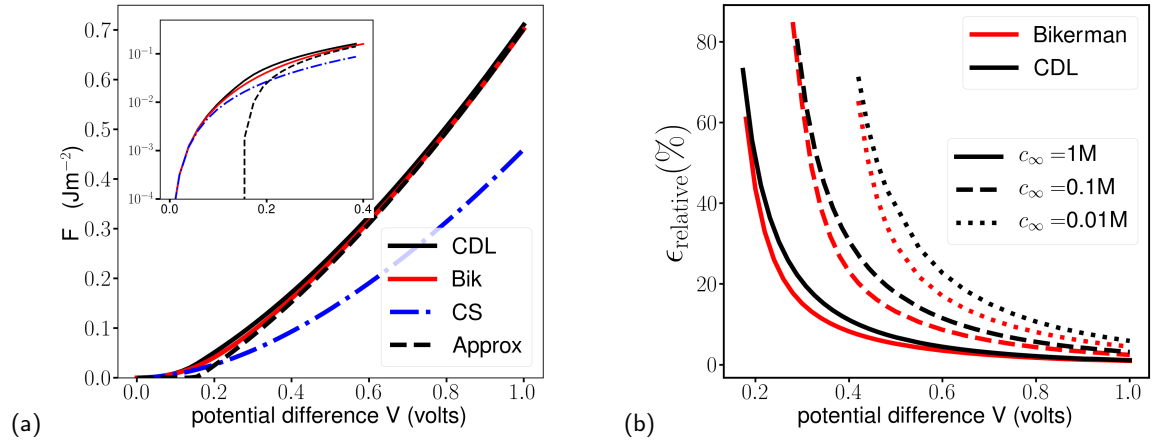

Figure 3: (a) Comparison of the total free energies of the CDL, Bikerman and CS models with the analytical approximation (b) Relative error of the analytical equations of the free energies to CDL and Bikerman model. 1M $LiPF_6$ used.

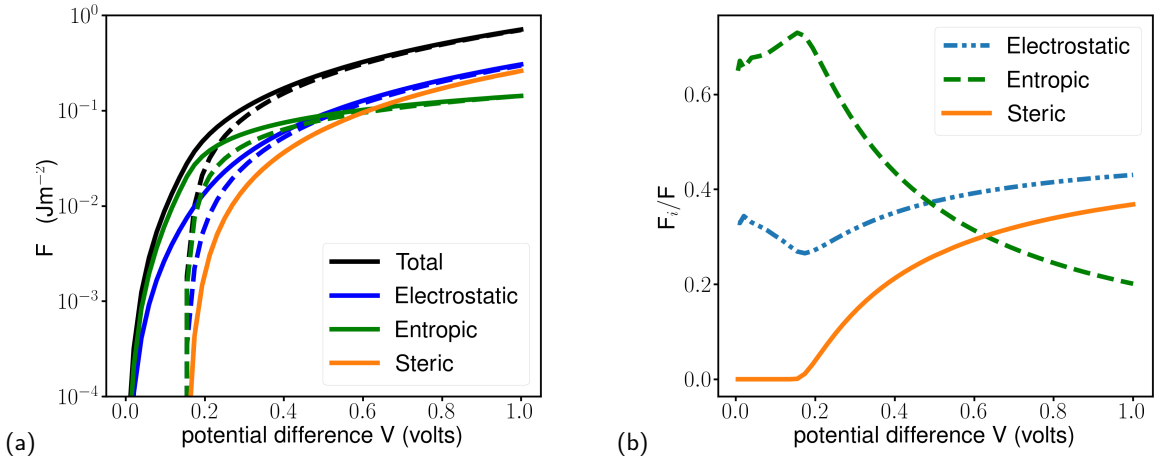

Figure 4: (a) Free energy components against potential difference. Solid lines are values from the CDL numerical solutions of equations Eqs. (8) to (10). The broken lines are the analytical approximations given by Eqs. (15) to (17). (b) The ratio of the components of the energy to the total energy. 1M $LiPF_6$ used.

the electrostatic chemical potential but opposite in sign, $\mu^{\text{st}} = -\mu^{\text{el}}$ which results in zero excess chemical potential, $\mu^{\text{ex}} = 0$. This leaves the concentration equal to the bulk everywhere in the solution. But a limiting value for the steric layer thickness can, applying the limiting value $\nu_\alpha = 2$, still be identified as $H = \sqrt{2\varepsilon_0\varepsilon_s\Phi_s/\rho^{\text{cap}}}$, with electrode charge density, $\sigma = \sqrt{2\varepsilon_0\varepsilon_s\rho^{\text{cap}}\Phi_s}$. The limiting capacitance then follows, $C = d\sigma/d\Phi_s = \varepsilon_0\varepsilon_s/H$. The same expression can be recovered for the capacitance from Eq.(6) under the limiting condition. In the limit of high bulk concentrations the free energy components, electrostatic and steric equally, reduce to $F_{\text{el,st}} = \Phi_{s\alpha}\sigma_\alpha/3 = k\Phi_{s\alpha}^{3/2}$. Here $k = \sqrt{2\varepsilon_0\varepsilon_s\rho^{\text{cap}}/9}$ is determined by the counterion, with concentration cap ρ^{cap}, and the solvent permittivity ε. The limiting total free energy at high concentration will then be the sum of those two free energies, $F = 2k\Phi_{s\alpha}^{3/2}$.

The effect of the ion size on the total free energy is generally known [46]. Our investigation confirmed that the smaller ion sizes provide higher energy, as shown in Fig.6. Anion specificity is clearly evident in both two-electrode (Fig.6a) and single-electrode energies (Fig.6b), though not surprisingly is stronger in the single-electrode case where anions alone serve as counterion. The anions form a typical Hofmeister series $Cl^- > BF_4^- > ClO_4^- > PF_6^-$. But it is

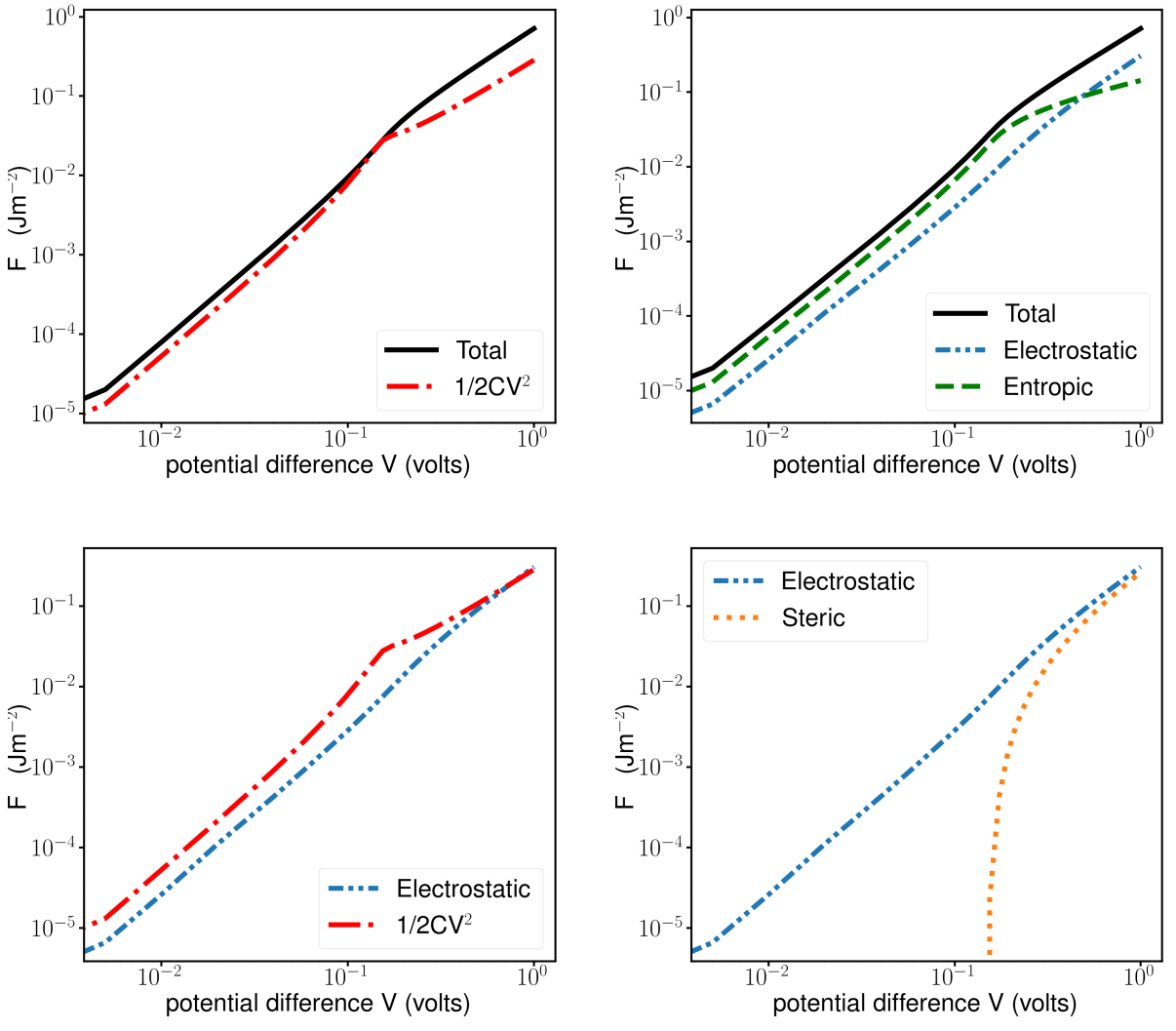

Figure 5: Free energy components of 1M $LiPF_6$. (Top left) total free energy curve against $\frac{1}{2}CV^2$. (Top right) total free energy curve against electrostatic and entropic components. (Bottom left) electrostatic energy component against $\frac{1}{2}CV^2$. (Bottom right) electrostatic energy against steric.

worth noting that this Hofmeister series is obtained solely through ion specific sizes, not through the ion dispersion forces commonly employed to interpret Hofmeister effects [40, 47]. The ion specificity here emerges at potential differences exceeding 0.2 V. We anticipate that ion dispersion forces would provide further ion specificity that may dominate at smaller potentials below 0.1 V.

In general, the steric chemical potential Eq.4 can be taken as a lower bound limit to that of the Bikerman and CS steric potentials, converging to the Bikerman model at large potential and concentrations. This lower steric potential leads to the build up of concentration relatively higher than the other models near the electrode, resulting in higher capacitance and energy in the system in comparison to the other steric models. Therefore, this model and the ensuing analytical approximations can provide an upper bound for the available energy in an electric double layer capacitors.

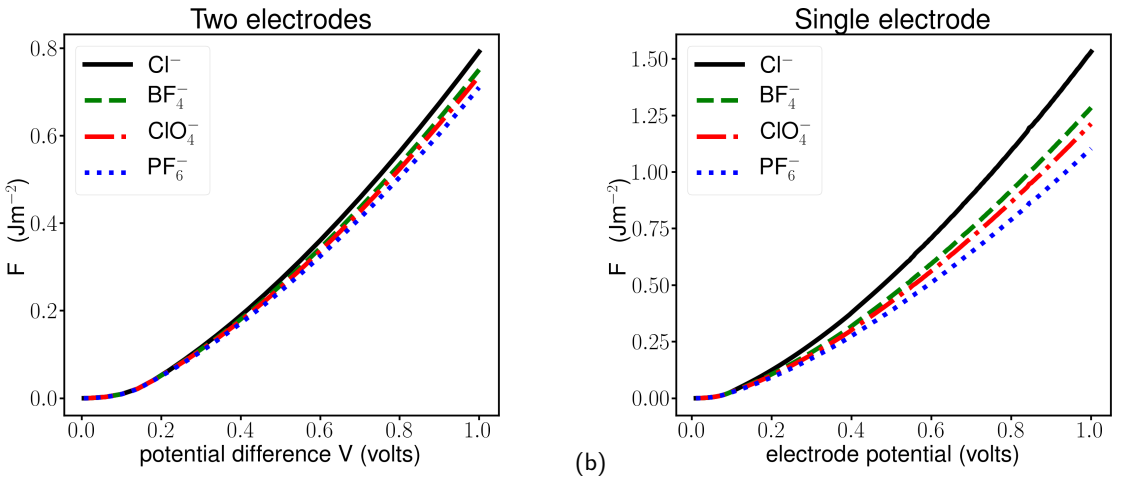

Figure 6: Total free energies of of 1M bulk concentration of LiCl, $LiBF_4$, $LiClO_4$ and $LiPF_6$ salts in PC solvent (a) in a two-electrode system against potential difference. (b) in a single electrode system against electrode potential.

5. Conclusion

We have applied an approximation for the steric chemical potential of a composite diffuse layer assuming the net resultant force on an ion is zero at thermal equilibrium. We then derived an analytical expression for the total free energy of EDLC. The analytical expression is given in terms of physical parameters of the ions, solvent and electrode potentials. This immensely simplifies our calculation of the energies without the need to solve a highly non-linear PB equation. And we have shown that at high potential both the CDL energies and the analytical approximation converges to the well known Bikerman free energies with relative error close to 1%. We have also shown that steric component has a vital contribution to the total free energy, which becomes comparable in magnitude to the electrostatic contribution at high voltages. $\frac{1}{2}CV^2$, which is widely used in determining the energy of an EDL capacitors from experimentally calculated capacitance, is also shown to be an oversimplified approach. We showed that the Carnahan-Starling model of steric interactions predicts a total free energy lower than the Bikerman model, but application of the CS model is impeded by its strongly nonlinear nature. The analytical expression presented here can therefore provide an upper bound for the available stored energy of a supercapacitor, and will prove useful in applications where it is not practical to numerically solve the nonlinearity of the Carnahan-Starling model.

Acknowledgements

The authors would like to acknowledge cloud computing resources provided through the Italian SuperComputing Resource Allocation administered by CINECA, and the Nimbus Cloud administered by the Pawsey Supercomputing Centre of Western Australia.

References

[1] Y. Bai, M. Greenfeld, K. J. Travers, V. B. Chu, J. Lipfert, S. Doniach, D. Herschlag, Quantitative and Comprehensive Decomposition of the Ion Atmosphere around Nucleic Acids, Journal of the American Chemical Society 129 (48) (2007) 14981–14988. doi:10.1021/ja075020g.

[2] E. Stellwagen, J. M. Muse, N. C. Stellwagen, Monovalent Cation Size and DNA Conformational Stability, Biochemistry 50 (15) (2011) 3084–3094. doi:10.1021/bi1015524.

[3] O. Stern, Zur Theorie der Elektrolytischen Doppelschicht, Z. Elektrochem. 30 (1924) 508. doi:10.1002/bbpc.192400182.

[4] J. J. Bikerman, Structure and capacity of electrical double layer, The London, Edinburgh, and Dublin Philosophical Magazine and Journal of Science 33 (220) (1942) 384–397. doi:10.1080/14786444208520813.

[5] M. Eigen, E. Wicke, The Thermodynamics of Electrolytes at Higher Concentration, The Journal of Physical Chemistry 58 (9) (1954) 702–714. doi:10.1021/j150519a007.

[6] N. F. Carnahan, K. E. Starling, Equation of State for Nonattracting Rigid Spheres, The Journal of Chemical Physics 51 (2) (1969) 635–636. doi:10.1063/1.1672048.

[7] T. Boublík, Hard-Sphere Equation of State, The Journal of Chemical Physics 53 (1) (1970) 471–472. doi:10.1063/1.1673824.

[8] G. A. Mansoori, N. F. Carnahan, K. E. Starling, T. W. Leland, Equilibrium Thermodynamic Properties of the Mixture of Hard Spheres, The Journal of Chemical Physics 54 (4) (1971) 1523–1525. doi:10.1063/1.1675048.

[9] I. Borukhov, D. Andelman, H. Orland, Steric Effects in Electrolytes: A Modified Poisson-Boltzmann Equation, Physical Review Letters 79 (3) (1997) 435–438. doi:10.1103/PhysRevLett.79.435.

[10] M. S. Kilic, M. Z. Bazant, A. Ajdari, Steric effects in the dynamics of electrolytes at large applied voltages. I. Double-layer charging, Phys. Rev. E 75 (2) (2007) 21502. doi:10.1103/PhysRevE.75.021502.

[11] A. A. Kornyshev, Double-Layer in Ionic Liquids: Paradigm Change?, The Journal of Physical Chemistry B 111 (20) (2007) 5545–5557. doi:10.1021/jp067857o.

[12] J. T. G. Overbeek, The role of energy and entropy in the electrical double layer, Colloids and Surfaces 51 (1990) 61–75. doi:DOI:10.1016/0166-6622(90)80132-N.

[13] V. Kralj-Iglic, A. Iglic, Influence of finite size of ions on electrostatic properties of electric double layer (1994).

[14] A. Kralj-Iglic, Veronika; Iglic, A Simple Statistical Mechanical Approach to the free Energy of the Electric Double Layer Including the Excluded Volume Effect, J.Phys. France 6 (1996) 477. doi:10.1051/jp2:1996193.

[15] K. Bohinc, A. Iglič, T. Slivnik, V. Kralj-Iglič, Charged cylindrical surfaces: Effect of finite ion size, Bioelectrochemistry 57 (1) (2002) 73–81. doi:10.1016/S1567-5394(01)00178-5.

[16] E. Ruckenstein, M. Manciu, The coupling between the hydration and double layer interactions, Langmuir 18 (20) (2002) 7584–7593. arXiv:https://doi.org/10.1021/la020435v, doi:10.1021/la020435v.

[17] D. Ben-Yaakov, D. Andelman, R. Podgornik, D. Harries, Ion-specific hydration effects: Extending the poisson-boltzmann theory, Current Opinion in Colloid Interface Science 16 (6) (2011) 542–550. doi:https://doi.org/10.1016/j.cocis.2011.04.012.

[18] D. L. Z. Caetano, G. V. Bossa, V. M. de Oliveira, M. A. Brown, S. J. de Carvalho, S. May, Role of ion hydration for the differential capacitance of an electric double layer, Phys. Chem. Chem. Phys. 18 (2016) 27796–27807. doi:10.1039/C6CP04199J.

[19] A. Warshel, M. Levitt, Theoretical studies of enzymic reactions: Dielectric, electrostatic and steric stabilization of the carbonium ion in the reaction of lysozyme, Journal of Molecular Biology 103 (2) (1976) 227–249. doi:https://doi.org/10.1016/0022-2836(76)90311-9.

[20] D. H. Mengistu, K. Bohinc, S. May, Poisson-boltzmann model in a solvent of interacting langevin dipoles, EPL (Europhysics Letters) 88 (1) (2009) 14003. doi:10.1209/0295-5075/88/14003.

[21] P. Koehl, H. Orland, M. Delarue, Beyond the poisson-boltzmann model: Modeling biomolecule-water and water-water interactions, Phys. Rev. Lett. 102 (2009) 087801. doi:10.1103/PhysRevLett.102.087801.

[22] D. Ben-Yaakov, D. Andelman, R. Podgornik, Dielectric decrement as a source of ion-specific effects, The Journal of Chemical Physics 134 (7) (2011) 074705. arXiv:https://doi.org/10.1063/1.3549915, doi:10.1063/1.3549915.

[23] J. J. López-García, J. Horno, C. Grosse, Poisson–boltzmann description of the electrical double layer including ion size effects, Langmuir 27 (23) (2011) 13970–13974, pMID: 22035520. arXiv:https://doi.org/10.1021/la2025445, doi:10.1021/la2025445.

[24] K. Bohinc, G. V. Bossa, S. May, Incorporation of ion and solvent structure into mean-field modeling of the electric double layer, Advances in Colloid and Interface Science 249 (2017) 220–233, recent nanotechnology and colloid science development for biomedical applications. doi:https://doi.org/10.1016/j.cis.2017.05.001.

[25] E. E. Fileti, Electric double layer formation and storing energy processes on graphene-based supercapacitors from electrical and thermodynamic perspectives, Journal of Molecular Modeling 26 (6) (2020) 159. doi:10.1007/s00894-020-04428-y.

[26] W. K. P. Wickramaarachchi, M. Minakshi, X. Gao, R. Dabare, K. W. Wong, Hierarchical porous carbon from mango seed husk for electrochemical energy storage, Chemical Engineering Journal Advances 8 (2021) 100158. doi:https://doi.org/10.1016/j.ceja.2021.100158.

[27] P. Sharma, M. Minakshi Sundaram, D. Singh, R. Ahuja, Highly energetic and stable gadolinium/bismuth molybdate with a fast reactive species, redox mechanism of aqueous electrolyte, ACS Applied Energy Materials 3 (12) (2020) 12385–12399. arXiv:https://doi.org/10.1021/acsaem.0c02380, doi:10.1021/acsaem.0c02380.

[28] M. Z. Bazant, M. S. Kilic, B. D. Storey, A. Ajdari, Towards an understanding of induced-charge electrokinetics at large applied voltages in concentrated solutions, Advances in Colloid and Interface Science 152 (1) (2009) 48–88. doi:10.1016/j.cis.2009.10.001.

[29] J. López-García, J. Horno, C. Grosse, Differential capacitance of the diffuse double layer at electrode-electrolyte interfaces considering ions as dielectric spheres: Part i. binary electrolyte solutions, Journal of Colloid and Interface Science 496 (2017) 531–539. doi:10.1016/j.jcis.2017.02.043.

[30] B. Giera, N. Henson, E. M. Kober, M. S. Shell, T. M. Squires, Electric double-layer structure in primitive model electrolytes: Comparing molecular dynamics with local-density approximations, Langmuir 31 (11) (2015) 3553–3562, pMID: 25723189. arXiv:https://doi.org/10.1021/la5048936, doi:10.1021/la5048936.

[31] R. Kjellander, Focus Article: Oscillatory and long-range monotonic exponential decays of electrostatic interactions in ionic liquids and other electrolytes: The significance of dielectric permittivity and renormalized charges, The Journal of Chemical Physics 148 (19) (2018) 193701. doi:10.1063/1.5010024.

[32] J. P. De Souza, K. Pivnic, M. Z. Bazant, M. Urbakh, A. A. Kornyshev, Structural Forces in Ionic Liquids: The Role of Ionic Size Asymmetry, Journal of Physical Chemistry B 2022 (2021) 1242–1253. doi:10.1021/ACS.JPCB.1C09441/SUPPL_FILE/JP1C09441_SI_001.PDF.

[33] K. Wojciechowski, Hydration energy or hydration force? Origin of ion-specificity in ion selective electrodes, Current Opinion in Colloid & Interface Science 16 (6) (2011) 601–606. doi:10.1016/j.cocis.2011.05.002.

[34] M. Kasuya, T. Sogawa, T. Masuda, T. Kamijo, K. Uosaki, K. Kurihara, Anion Adsorption on Gold Electrodes Studied by Electrochemical Surface Forces Measurement, The Journal of Physical Chemistry C 120 (29) (2016) 15986–15992. doi:10.1021/acs.jpcc.5b12683.

[35] D. F. Parsons, B. W. Ninham, Ab Initio Molar Volumes and Gaussian Radii, The Journal of Physical Chemistry A 113 (6) (2009) 1141–1150. doi:10.1021/jp802984b.

[36] J. M. Borah, S. Mahiuddin, N. Sarma, D. F. Parsons, B. W. Ninham, Specific Ion Effects on Adsorption at the Solid/Electrolyte Interface: A Probe into the Concentration Limit, Langmuir 27 (14) (2011) 8710–8717. doi:10.1021/la2006277.

[37] D. F. Parsons, The impact of nonelectrostatic physisorption of ions on free energies and forces between redox electrodes: ion-specific repulsive peaks, Electrochimica Acta 189 (2016) 137–146. doi:10.1016/j.electacta.2015.12.090.

[38] D. F. Parsons, B. W. Ninham, Nonelectrostatic Ionic Forces between Dissimilar Surfaces: A Mechanism for Colloid Separation, The Journal of Physical Chemistry C 116 (14) (2012) 7782–7792. doi:10.1021/jp212154c.

[39] C. G. Gray, P. J. Stiles, Nonlinear electrostatics: the Poisson–Boltzmann equation, European Journal of Physics 39 (5) (2018) 53002. doi:10.1088/1361-6404/aaca5a.

[40] D. F. Parsons, Supercapacitors have an asymmetric electrode potential and charge due to nonelectrostatic electrolyte interactions, Colloids and Surfaces A: Physicochemical and Engineering Aspects 460 (2014) 51–59. doi:10.1016/j.colsurfa.2014.01.084.

[41] L. Yang, B. H. Fishbine, A. Migliori, L. R. Pratt, Dielectric saturation of liquid propylene carbonate in electrical energy storage applications, The Journal of Chemical Physics 132 (4) (2010) 044701. arXiv:https://doi.org/10.1063/1.3294560, doi:10.1063/1.3294560.

[42] M. S. Alnæs, J. Blechta, J. Hake, A. Johansson, B. Kehlet, A. Logg, C. Richardson, J. Ring, M. E. Rognes, G. N. Wells, The FEniCS Project Version 1.5, Archive of Numerical Software 3 (100) (2015). doi:10.11588/ans.2015.100.20553.

[43] Bossa, Guilherme V., Caetano, Daniel L. Z., de Carvalho, Sidney J., Bohinc, Klemen, May, Sylvio, Modeling the camel-to-bell shape transition of the differential capacitance using mean-field theory and monte carlo simulations, Eur. Phys. J. E 41 (9) (2018) 113. doi:10.1140/epje/i2018-11723-7.

[44] M. Chen, W. Dou, S. Zhou, Fast newton iterative method for local steric poisson–boltzmann theories in biomolecular solvation (2021). doi:10.48550/ARXIV.2111.00834.
URL https://arxiv.org/abs/2111.00834

[45] D. F. Parsons, Predicting ion specific capacitances of supercapacitors due to quantum ionic interactions, Journal of Colloid and Interface Science 427 (2014) 67–72. doi:10.1016/j.jcis.2014.01.018.

[46] S. Zhou, How ion size influences energy storage in cylindrical nanoporous supercapacitors, The Journal of Physical Chemistry C 123 (49) (2019) 29638–29646. arXiv:https://doi.org/10.1021/acs.jpcc.9b10215, doi:10.1021/acs.jpcc.9b10215.

[47] A. Salis, B. W. Ninham, Models and mechanisms of Hofmeister effects in electrolyte solutions, and colloid and protein systems revisited, Chem. Soc. Rev. 43 (21) (2014) 7358–7377. doi:10.1039/C4CS00144C.